

## Force distributions in three-dimensional compressible granular packs

J. Michael Erikson, Nathan W. Mueggenburg, Heinrich M. Jaeger, and Sidney R. Nagel

*The James Franck Institute and Department of Physics, The University of Chicago, 5640 South Ellis Avenue, Chicago, Illinois 60637*

(Received 5 June 2002; published 14 October 2002)

We present an experimental investigation of the probability distribution of normal contact forces,  $P(F)$ , at the bottom boundary of static three-dimensional packings of compressible granular materials. We find that the degree of deformation of individual grains plays a large role in determining the form of this distribution. For small amounts of deformation we find a small peak in  $P(F)$  below the mean force with an exponential tail for forces larger than the mean force. As the degree of deformation is increased the peak at the mean force grows in height and the slope of the exponential tail increases.

DOI: 10.1103/PhysRevE.66.040301

PACS number(s): 81.05.Rm, 83.80.Fg, 45.70.Cc

It is known that forces within a granular material are distributed in a highly inhomogeneous manner [1]. The largest interparticle forces are arranged in a network of force chains, while other particles are shielded from the external force [2–6]. One quantitative way of analyzing the inhomogeneities of these force networks is to measure the probability distribution,  $P(F)$ , of normal forces,  $F$ , between neighboring particles.

Experiments have shown that under a wide range of parameters,  $P(F)$  at the boundaries of granular packs decays exponentially for forces larger than the mean force,  $\bar{F}$ , and has a small peak near the mean force [by “small” we mean that  $P(F)$  increases by less than a factor of two between its minimum near  $F=0$  and the peak] [6–11]. This form of  $P(F)$  has been found to be independent of interparticle friction and the texture (geometrical ordering) of the granular pack. Based upon granular simulations and theoretical work it is expected that the form of  $P(F)$  should depend strongly on the amount of deformation of the individual grains [11–14], with a crossover to Gaussian behavior at high deformations. Furthermore, simulations of supercooled liquids (i.e., frictionless particles) by O’Hern *et al.* suggest that the exponential tail in  $P(F)$  might arise from a self-averaging of configurations with different average forces [15,16]. As the packing fraction is increased, corresponding to greater deformations, they find that the relative fluctuations in the average force decrease, leading to a Gaussian form of  $P(F)$  when using a Hooke’s law potential of interaction.

Simulations by Snoeijer *et al.* suggest that the form of the force distribution within a granular pack may be very sensitive to the number of contacts between grains with a larger number of contacts leading to a large peak in  $P(f)$  and steeper exponential decay at large forces [19]. It is expected that this coordination number should increase substantially as the deformation of the grains is increased, and thus any effect on the probability distribution of forces should be detected.

Experimentally it has been difficult to measure the force distribution of compressible materials. In 2D shear experiments Howell *et al.* find a transition to Gaussian behavior for deformations of the order of 2% [17,18]. In 3D static packings Makse *et al.* have reported some experimental evidence for a transition from pure exponential to Gaussian. However, their maximum deformations were only of the order of 0.4%

[11] and conflict with the measurements of Blair *et al.* at similar deformations [8] and with the work of Løvøll *et al.* at very low amounts of deformation [9].

We present an experimental investigation of the probability distribution of normal forces at the boundaries of granular packs over a wide range of deformations. For average particle deformations up to approximately 30% we find a form of  $P(F)$  similar to that found in previous experiments at low deformations as in Refs. [7–9]. For large deformations (of the order of 40%) we find that  $P(F)$  shows a much more pronounced peak around the mean force, but interestingly, we do not find Gaussian behavior for large deformations.

Rubber beads of three different hardnesses (40, 50, and 60 durometer; hereafter referred to as soft, medium, and hard respectively) with diameters  $3.12 \pm 0.05$  mm were contained within an acrylic cylinder of inner diameter 140 mm. Amorphous packings approximately 72 mm in height were bounded on the top and bottom by close fitting acrylic disks. The packs of rubber beads were constructed with one layer of glass beads at the bottom surface in a crystalline arrangement. Rubber beads were added on top of the glass layer slowly so as not to disturb the underlying glass particles. The normal forces of the individual glass beads at the bottom surface were measured using the carbon paper method [6–8,20]. In this way the layer of glass beads acted as an array of force transducers which could be easily calibrated.

The experiments were performed by applying a force of between 2500N and 7000N to the top piston of the cell with a hydraulic press. The normal forces between individual glass beads in the bottom layer and the bottom piston were measured by placing carbon paper and white paper [21] between the pack and the bottom piston. The size and intensity of the mark left on the white paper depended on the magnitude of the normal force on the corresponding glass bead.

Following each experiment the white paper was carefully removed and digitized with a flat bed scanner. The images were then processed using image analysis software to find the area and intensity of each mark. The intensities of the marks were converted to the force on the corresponding bead using a fourth order polynomial interpolation of calibration data as explained in Ref. [8]. An appropriate number was added to the lowest bin to account for beads with forces too small to leave a resolvable mark. Since the bottom layer was crystalline, the total number of contacts was known and

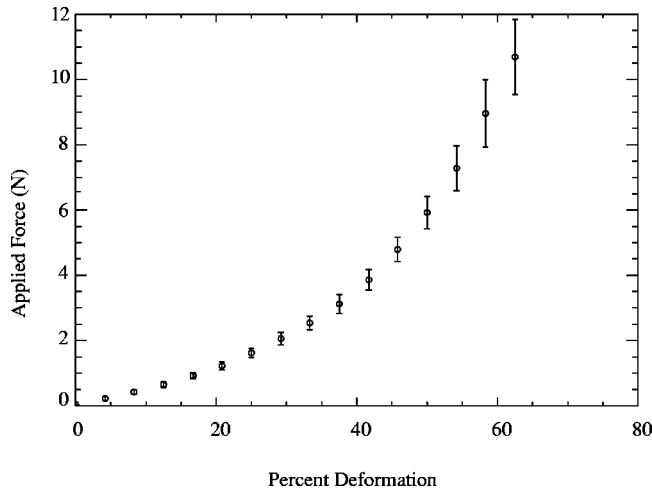


FIG. 1. Force versus deformation for soft rubber particles. The applied compressional force versus percent deformation for individual soft rubber particles compressed between two plates. Error bars represent the standard deviation of multiple measurements.

agreed well with the number of observed contacts at high applied forces. All forces for a given experimental run were normalized to the average force for that run and the resulting probability distribution,  $P(f)$ , of normalized forces,  $f = F/\bar{F}$ , was averaged over 4 to 11 independent experimental runs. Each run provided approximately 1500 imprints. This results in a noise floor of approximately 0.002 to 0.003 in  $P(f)$  shown below.

The degree of deformation of individual grains was estimated by measuring the compression of individual grains in response to a known force between two plates. The percent change in size along the direction of the applied force was recorded as a function of force for the three different hardnesses of rubber beads and for the glass beads. Figure 1 shows the applied force versus percent of deformation for the soft rubber particles.

In order to compare our results with the earlier work of Mueth *et al.* and Blair *et al.* we examined amorphous packings of smooth spherical soda lime glass beads of diameter  $3.06 \pm 0.04$  mm. Figure 2(a) shows the probability distribution of normal forces,  $P(f)$ , at the bottom boundary averaged over four experimental runs with an average force of 3.0N per bead. This average force applied to an individual glass bead results in a deformation of less than 2%. We find an exponential decay for large forces and a small peak in the distribution near the mean force, consistent with previous experimental results [7–9].

Experiments were next done with amorphous packs of rubber beads. Figures 2(b) 2(c), and 2(d) show the probability distributions of normal forces at the bottom boundary for three different hardnesses of beads with approximately the same average force. The hard and medium rubber packings show a distribution of forces below the mean force similar to that of the glass beads, and exhibit an exponential decay for forces larger than the mean force. The shape of the distribution did not change significantly, however the slopes of  $-1.6$  and  $-1.9$  respectively are somewhat larger than the slope of  $-1.1$  for the glass bead packings. The soft rubber

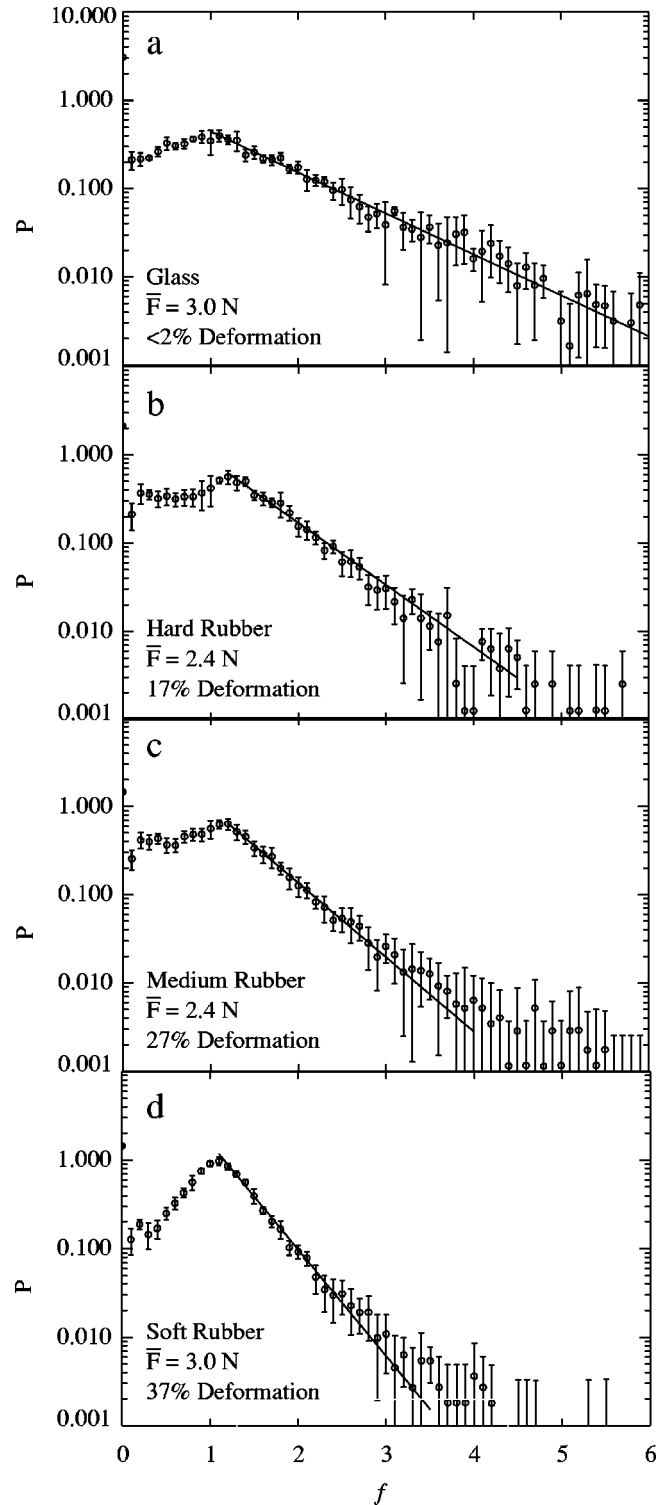


FIG. 2.  $P(f)$  with varying particle hardness. Probability distribution of normal forces at the bottom boundary of amorphous packing of (a) glass, (b) hard rubber, (c) medium rubber, and (d) soft rubber beads. Each plot represents an average of 4 to 11 experimental runs. The average force per bead,  $\bar{F}$ , and the deformation of an individual bead under this applied force are indicated. Error bars represent statistical deviations from multiple experimental realizations. The solid line is a fit to an exponential over the large force region resulting in slopes listed in Table I.

TABLE I. Exponential decay constants for  $P(f)$  at large forces and peak size as explained in the text for various types of beads at various levels of forcing and deformation of individual beads.

Bead type	$\bar{F}$ (N)	Deformation (%)	Slope	Peak size
Glass	3.0	<2	-1.1	1.9
Hard rubber	2.4	17	-1.6	1.8
Medium rubber	2.4	27	-1.9	2.0
Soft rubber	3.0	37	-2.8	6.0
Soft rubber	1.6	25	-2.4	1.8
Soft rubber	2.0	30	-2.6	2.0
Soft rubber	3.0	37	-2.8	6.0
Soft rubber	4.4	45	-3.8	29

bead packings, which had a larger amount of deformation, show a significantly more pronounced peak and a steeper decay. The deformation reported is for a single bead with the average force  $\bar{F}$  applied to it. Using Fig. 1 one can estimate the deformation of beads at different values of  $f$ . The region near the peak remains exponential with a slope of  $-2.8$ , while above  $f=2$  the distribution begins to depart from exponential behavior. Table I shows the exponential decay constants for  $P(f)$  at large forces and the size of the peaks as characterized by the maximum height of the peak divided by the minimum value of a smooth fit to the distribution between  $f=0.1$  and  $f=0.7$ .

Note that changes in the calculated peak height are a good indicator for changes in the overall shape of  $P(f)$ . From Table I we see that significant changes in peak height occur when the average deformation of individual particles exceeds roughly 30%.

To check this trend more directly, we performed the same experiments for a single type of bead (soft rubber) with varying amounts of pressure as shown in Fig. 3. As before, the slope of  $P(f)$  remains essentially unchanged (the peak height does not exceed a value of 2) until the average degree of deformation exceeds roughly 30%. Beyond this amount of deformation, the peak size increases sharply and  $P(f)$  evolves into a much more symmetric form [Figs. 3(c) and 3(d)]. Remarkably this evolution in the shape of  $P(f)$  does not seem to be connected with a transition to Gaussian behavior. Near the peak, the distribution is well fit to an exponential decay (see fitted lines in Figs. 2 and 3). With a larger bin width it is possible to increase the accuracy of data in the high force regime at the sacrifice of data density. In this way it has been determined that at the largest deformations [see Fig. 3(d)] the large force tail of  $P(f)$  is even slower than exponential, and shows the opposite trend to what would be expected if the distribution was to revert to a Gaussian profile at large deformations.

An intriguing question is to what extent the force distribution of the highly compressed rubber packings resembles that of a homogeneous block of rubber. The inset of Fig. 3(d) compares data from the main panel to a fit to data from a control experiment performed on a block of rubber on top of a single layer of glass beads. The width of this fitted distri-

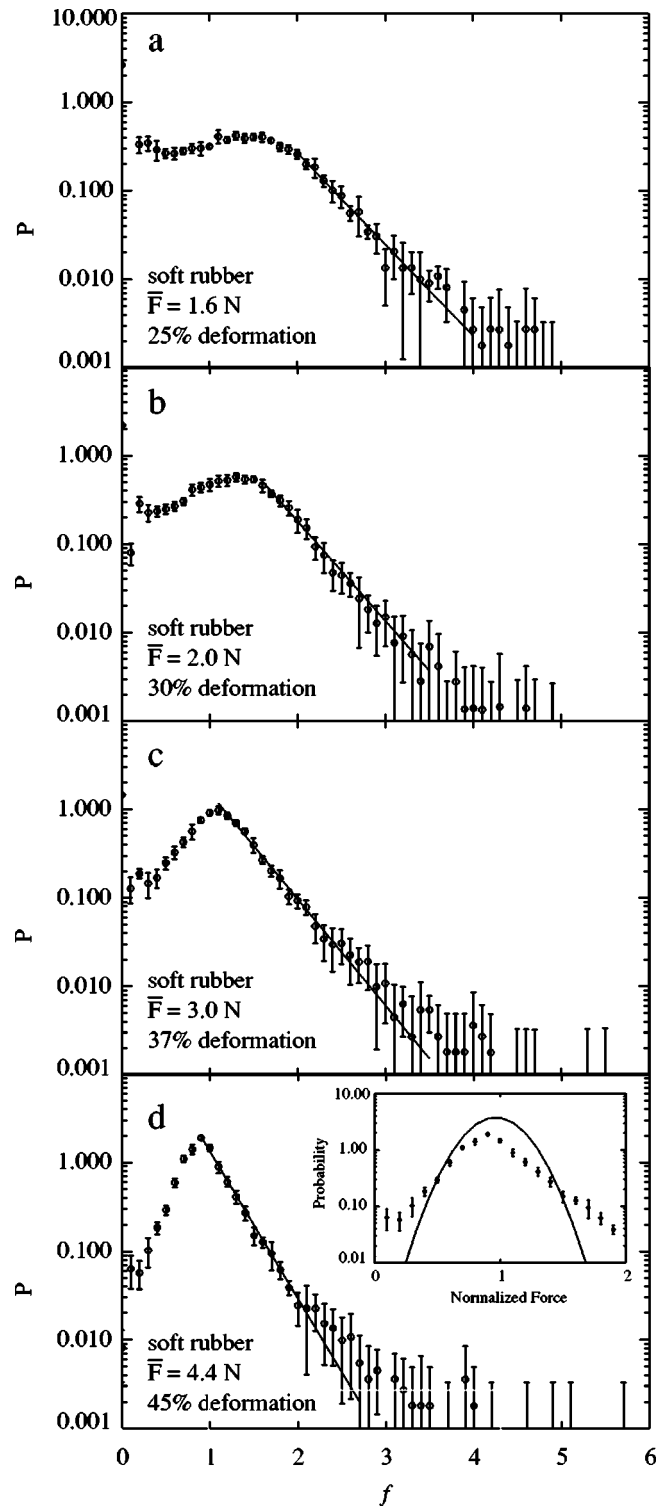


FIG. 3.  $P(f)$  with varying applied force. Probability distributions of normal forces at the bottom boundary of amorphous packings of soft rubber beads. Each plot represents an average over 7 to 9 experimental runs. Part (c) is equivalent to Fig. 2(d). The error bars represent statistical variations among experimental runs. The solid lines are fit to exponentials over the large force region. The inset of (d) compares the data to the Gaussian form obtained from a fit to  $P(f)$  of a control experiment taken with a block of rubber on top of a single layer of glass beads.

bution is due to the resolution of the carbon paper technique. Note that at large deformations the force distribution from a pack of rubber beads does not resemble that of a rubber block, and in particular the distribution of forces from a pack of rubber beads is significantly broader than that of a rubber block. Because of the limitations of the carbon paper technique we are unable to rule out any residual influence of the single layer of glass beads on the final shape of  $P(f)$ . However, regardless of the effect on the exact form of the probability distribution, any observed changes in this distribution as the type of rubber bead is changed or as the amount of deformation is increased must be connected to properties of the rubber packing itself.

We find that the degree of deformation of individual particles does play a large role in determining the form of the probability distribution of forces within a granular pack. When the degree of deformation is small, either with hard particles or with soft particles under a small force, we find that  $P(f)$  has an exponential decay for forces larger than the mean force and a small peak near the mean force, consistent

with previous experimental investigations [6–11]. As the average amount of deformation of individual beads increases beyond approximately 30%, the peak near the mean force grows more pronounced. This peaking behavior is in agreement with simulations, although at higher deformations than would have been expected [11–15,19]. For forces larger than the mean force, we do not see a Gaussian decay. The distribution continues to decay exponentially (or even slower) at large forces. The slope of the exponential decay does increase with deformation in agreement with the predictions of increasing coordination number of Snoeijer *et al.*, but it is still not clear why this effect does not occur for smaller amounts of deformation [19].

We thank A. Bushmaker, E. Corwin, A. Marshall, M. Möbius, and D. Mueth for their assistance with this project. This work was supported by NSF under Grant No. CTS-9710991, by the MRSEC Program of the NSF under Grant No. DMR-9808595, and by the MRSEC REU program at The University of Chicago.

- 
- [1] H.M. Jaeger, S.R. Nagel, and R.P. Behringer, *Phys. Today* **49**, 32 (1996); *Rev. Mod. Phys.* **68**, 1259 (1996).
- [2] P. Dantu, in *Proceedings of the 4th International Conference On Soil Mechanics and Foundation Engineering*, London, 1957 (Butterworths, London, 1958), Vol. 1, pp. 144–148.
- [3] P. Dantu, *Ann. Ponts Chaussees* **IV**, 193 (1967).
- [4] D. Howell and R. P. Behringer, in *Powders & Grains 97*, edited by R. P. Behringer and J. T. Jenkins (Balkema, Rotterdam, 1997), pp. 337–340.
- [5] M. Ammi, D. Bideau, and J.P. Troadec, *J. Phys. D* **20**, 424 (1987).
- [6] C.-h. Liu, S.R. Nagel, D.A. Schecter, S.N. Coppersmith, S. Majumdar, O. Narayan, and T.A. Witten, *Science* **269**, 513 (1995).
- [7] D.M. Mueth, H.M. Jaeger, and S.R. Nagel, *Phys. Rev. E* **57**, 3164 (1998).
- [8] D.L. Blair, N.W. Mueggenburg, A.H. Marshall, H.M. Jaeger, and S.R. Nagel, *Phys. Rev. E* **63**, 041304 (2001).
- [9] G. Lóvvoll, K.N. Málkóy, and E.G. Flekkóy, *Phys. Rev. E* **60**, 5872 (1999).
- [10] G. W. Baxter, in *Powders & Grains 97* (Ref. [9]), pp. 345–348.
- [11] H.A. Makse, D.L. Johnson, and L.M. Schwartz, *Phys. Rev. Lett.* **84**, 4160 (2000).
- [12] C. Thornton, *Kona* **15**, 81 (1997).
- [13] C. Thornton and S.J. Antony, *Philos. Trans. R. Soc. London, Ser. A* **356**, 2763 (1998).
- [14] M.L. Nguyen and S.N. Coppersmith, *Phys. Rev. E* **62**, 5248 (2000).
- [15] C.S. O’Hern, S.A. Langer, A.J. Liu, and S.R. Nagel, *Phys. Rev. Lett.* **86**, 111 (2001).
- [16] C. S. O’Hern, S. A. Langer, A. J. Liu, and S. R. Nagel, *Phys. Rev. Lett.* **88**, 075507 (2002).
- [17] D. Howell, R.P. Behringer, and C. Veje, *Phys. Rev. Lett.* **82**, 5241 (1999).
- [18] D. Howell (private communication); R. Behringer (private communication).
- [19] J. Snoeijer, M. van Hecke, E. Somfai, and W. van Saarloos, e-print cond-mat/0204277.
- [20] F. Delyon, D. Dufresne, and Y.-E. Lévy, *Ann. Ponts Chaussees* **22**, (1990).
- [21] We used Super Nu-Kote SNK-11 1/2 carbon paper and Hammermill Laser Print Long Grain Radiant White paper.